CHAPTER II

BACKGROUND AND LITERATURE REVIEW

2.1 Photocatalysis theory

Photocatalysis can be defined as an acceleration of a reaction in the presence of an irradiated catalyst. There are two types of photocatalysis: homogeneous and heterogeneous. Homogeneous photocatalysis uses the same phase for the contaminant substrate and the catalyst as illustrated by the degradation of an organic compound in the presence of ferrous ions and H_2O_2. By way of contrast, heterogeneous photocatalysis involves different phases for the contaminant substrate, and the catalyst as exemplified by the degradation of an organic compound in the liquid phase in the presence of (solid) titanium dioxide and UV light.

Semiconductors are considered as practicable materials for use as catalysts in photocatalytic reactions. In general, semiconductors are characterized by a valence band and a conduction band which are separated by an energy gap as shown in Figure 2.1. When semiconductors absorb light with energy equal to, or higher than, this bandgap, electrons are excited from the valence band to the conduction band. This excitation of electrons generates electron vacancies in the valence band, which are called holes. The excited electron in the conduction band and the resulting hole in the valence band are called an "electron-hole pair". The electrons and holes that survive recombination play a crucial part for pollutant removal by heterogeneous photocatalysis.

It is interesting that the oxidizing power of the photogenerated holes in the valence band of a semiconductor is greater than the reducing power of the excited electrons in the conduction band (Rajeshwar, 1995). When water molecules (or hydroxyl groups) are adsorbed on the surface of a semiconductor, they are oxidized by the photogenerated holes and hydroxyl radicals ($OH^{\bullet}$) are formed:

$$OH^- + h^+_{VB} \xrightarrow[h\nu]{SC} OH^{\bullet}$$

where SC represents a semiconductor and h^+_{VB} represents a photogenerated hole. These highly reactive radicals can be used to mineralize, or at least partially degrade, most organic contaminants. The $OH^\bullet$ radicals are also non-selective in their attack of microorganisms and cause cell deactivation in many cases.

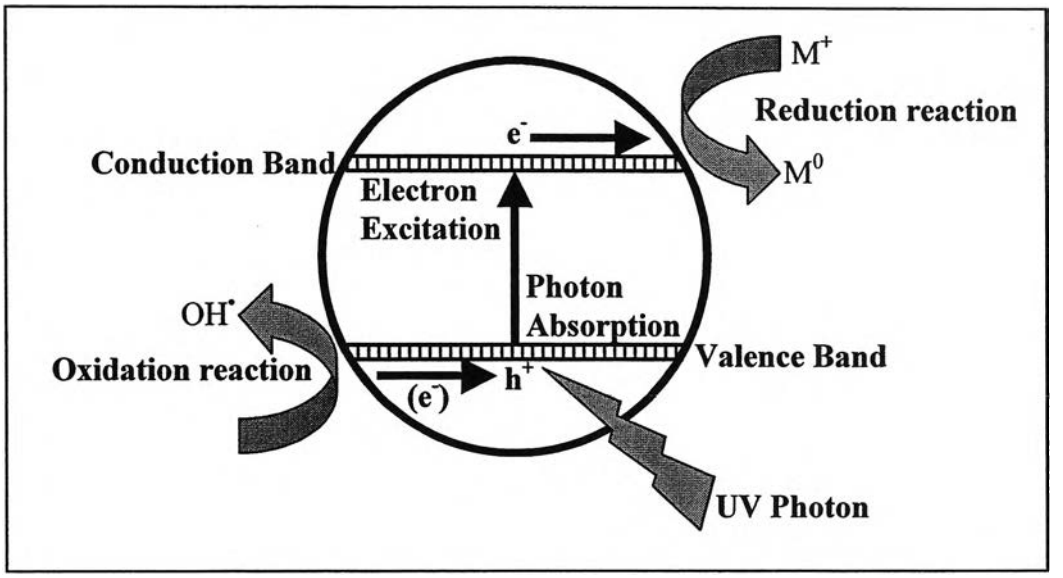

Figure 2.1 Schematic of the photocatalytic process in a semiconductor

In addition, photocatalytic oxidation of metal ions is possible via photogenerated holes. The reaction occurres when the reduction potential of the metal ion is less positive than the potential corresponding to the valence band edge of the semiconductor. In this process, oxygen gas is provided to the aqueous titania suspensions, and it plays the role as an electron acceptor and produces O_2^- species. The metal ions are oxidized either by the holes (h^+) or by the O_2^- species to the corresponding oxides, and are deposited on the surface of the semiconductor. In the case of metal ions with relatively high negative reduction potentials such as Pb(II) or Mn(II), the direct photocatalytic reduction pathway is prohibited or becomes very difficult. The oxidation pathway through photogenerated holes is possible due to the existence of stable higher oxidation states for these metallic species (Rajeshwar and Ibanez, 1997).

In the same manner, photogenerated electrons can be used for a variety of reduction reactions. In the presence of oxygen, the photogenerated electrons can reduce oxygen to a superoxide radical anion ($O_2^{\bullet -}$). These radicals can decompose the organic contaminants to carbon dioxide and water. In contrast, without oxygen, the

photogenerated electrons tend to combine with other electron acceptors such as metal ions already present in the water. Thus, the metal ions, M^{n+}, can be reduced to their elemental form, M^0, as exemplified by Equation 2.1:

$$M^{n+}_{(aq)} + ne^-_{CB} \xrightarrow[h\nu]{SC} M^0_{(s)} \qquad (2.1)$$

where e^-_{CB} represents a photogenerated electron. They can also be converted to an environmentally more benign oxidation state. The photocatalytic reduction process is thermodynamically possible for metal ions with a reduction potential more positive than the potential corresponding to the conduction band edge of the semiconductor. For example, the metal ions which can be removed by this method include Ag(I), Cu(II), Hg(II) and Cr(VI).

2.1.1 Kinetic considerations in heterogeneous photocatalysis

The Langmuir-Hinshelwood model is widely used to analyze the disappearance rate of contaminants in water, especially in the presence of pre-adsorption or dark adsorption prior to illumination. The Langmuir adsorption model assumes that:

(1) at equilibrium, the number of surface adsorption sites is fixed
(2) only one substrate may bind at each surface site
(3) the heat of adsorption for the substrate is identical for each site and is independent of surface coverage
(4) there is no interaction between adjacent adsorbed molecules
(5) the rate of surface adsorption of the substrate is greater than the rate of any subsequent chemical reactions
(6) there is no irreversible blocking of active sites by binding to product.

With these assumptions, the surface coverage, θ, is related to the initial concentration of the substrate, C, and to the apparent adsorption equilibrium constant, K, via the following equation:

$$\theta = \frac{KC}{(1+KC)} \qquad (2.2)$$

The rate of product formation can then be written as a single-component Langmuir-Hinshelwood expression:

$$r = -\frac{dC}{dt} = \frac{kKC}{(1+KC)} \tag{2.3}$$

where r represents the initial rate of disappearance of the contaminant, k is an apparent reaction rate constant which is related to the adsorption/desorption affinity, and K is the Langmuir constant reflecting the adsorption/desorption equilibrium between the reagent and the surface of the photocatalyst.

A convenient means of using this equation is to demonstrate linearity of the data when plotted as the inverse initial rate ($1/r$) versus inverse initial concentration ($1/C$):

$$\frac{1}{r} = \frac{1}{k} + \frac{1}{kKC} \tag{2.4}$$

with both slope ($1/kK$) and intercept ($1/k$) positive.

For low levels of contaminants, the reaction rate is essentially of the first order:

$$r = kKC \tag{2.5}$$

In this scenario, the apparent reactivity of a molecule is the product of two characteristics; the rate constant, k, and the Langmuir constant, K.

In general, the highest efficiency of the photocatalytic degradation will be observed at a relatively high concentrations of substrate to satisfy the condition $KC >>> 1$ in Equation 2.3. (Emeline et al., 2000). Turchi and Ollis (1990) reported that the apparent constant K represents different combinations of the Langmuir constant, carrier trapping constants, and surface reaction constants, all of which are important to achieve a higher efficiency for the photocatalyst. Cunningham and Al-Sayyed (1990) have measured dark Langmuir adsorption isotherms for TiO_2 for a

variety of different organic pollutants, and the values of K are significantly smaller than the values of K obtained from plots of $1/r$ versus $1/C$.

The rate constant, k, depends on the light intensity. At low photon intensity, k scales linearly with light intensity, whereas at higher light intensity, it scales with the square root of the light intensity. From Equation 2.5, as $KC>>>1$, the reaction rate, r, is dependent on k and, consequently, the light intensity. The dependence of reaction rate on light intensity can be illustrated as the following equations:

low light intensity, $r \alpha I$ (2.6)

high light intensity, $r \alpha I^{1/2}$ (2.7)

very high light intensity, $r \alpha I^0$ (independent) (2.8)

where I represents the incident light intensity.

Two explanations have been put forward for the square-root dependence. First, the carrier recombination is thought to dominate at the higher light intensities (Okamoto et al., 1985), and secondly, the occurrence of bimolecular recombination of $OH^{\bullet}$ can also account for this dependence (Kormann et al., 1991). The independence of the reaction rate on a very high light intensity can be explained in terms of a diffusion limitation on the transport of the reagent molecules to the photocatalyst surface (Emeline et al., 2000).

2.2 Titanium dioxide

TiO_2 mediated photocatalytic reactions are gaining nowadays more and more importance and this is reflected in the increasing number of publications that relate to theoretical aspects and practical applications of these reactions as shown in Figure 2.2.

Titanium dioxide, TiO_2, is considered the most practical material among the semiconductors used in photocatalysis due to its exceptional stability. It is stable upon illumination and has low solubility and corrosion during photocatalysis. TiO_2 exists in three different crystal structures: rutile, anatase, and brookite (Linsebigler et al., 1995). Rutile and anatase have been used as catalysts in heterogeneous photocatalysis while brookite is not commonly available. The photoactivity of these two crystals mainly depends on their structure (Linsebigler et al., 1995). Both rutile and anatase

structures can be described as chains of octahedra. The two crystal structures differ by the distortion of each octahedron and by the assembly pattern of octahedral chains.

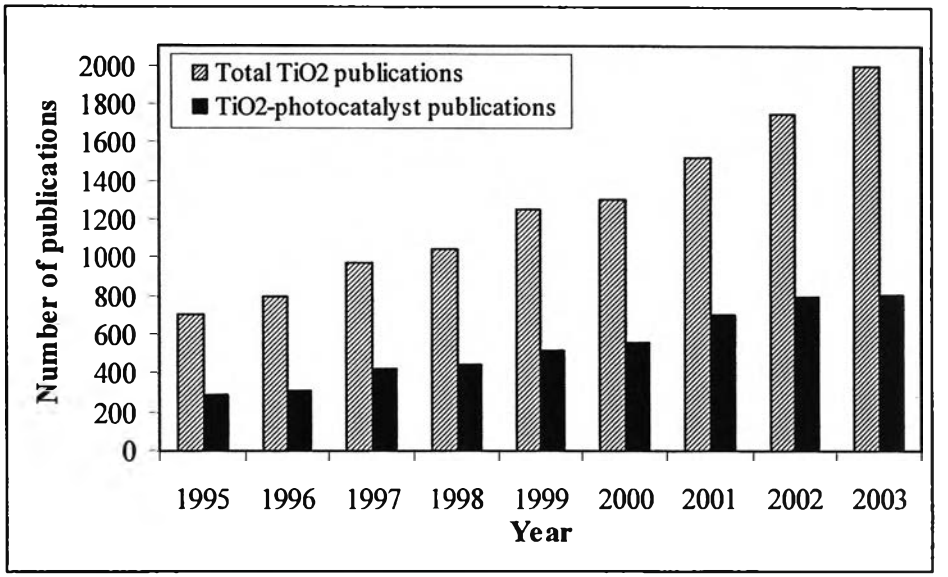

Figure 2.2 Number of publications regarding TiO_2/TiO_2-photocatalysis per year (ISI-CD source, adapted from Carp et al., 2004)

Figure 2.3 shows the crystal structure of rutile and anatase. Each Ti^{4+} is surrounded by an octahedron of six O^{2-} ions; the octahedron in rutile is slightly distorted. The octahedron in anatase is significantly more distorted so that its symmetry is lower than orthorhombic. The Ti-Ti distances in anatase are greater (3.79 Å and 3.04 Å versus 3.57 Å and 2.96 Å in rutile) whereas the Ti-O distances are shorter in rutile (1.934 Å and 1.980 Å in anatase versus 1.949 Å and 1.980 Å in rutile). In the rutile structure, each octahedron is in contact with ten neighboring octahedra (two sharing edge oxygen pairs and eight sharing corner oxygen atoms). In the anatase structure, each octahedron is in contact with eight neighbors (four sharing an edge and four sharing a corner). These differences in lattice structure cause different mass densities and electronic band structures between the two forms of TiO_2 as indicated in Table 2.1 (Linsebigler et al., 1995; Fujishima et al., 1999).

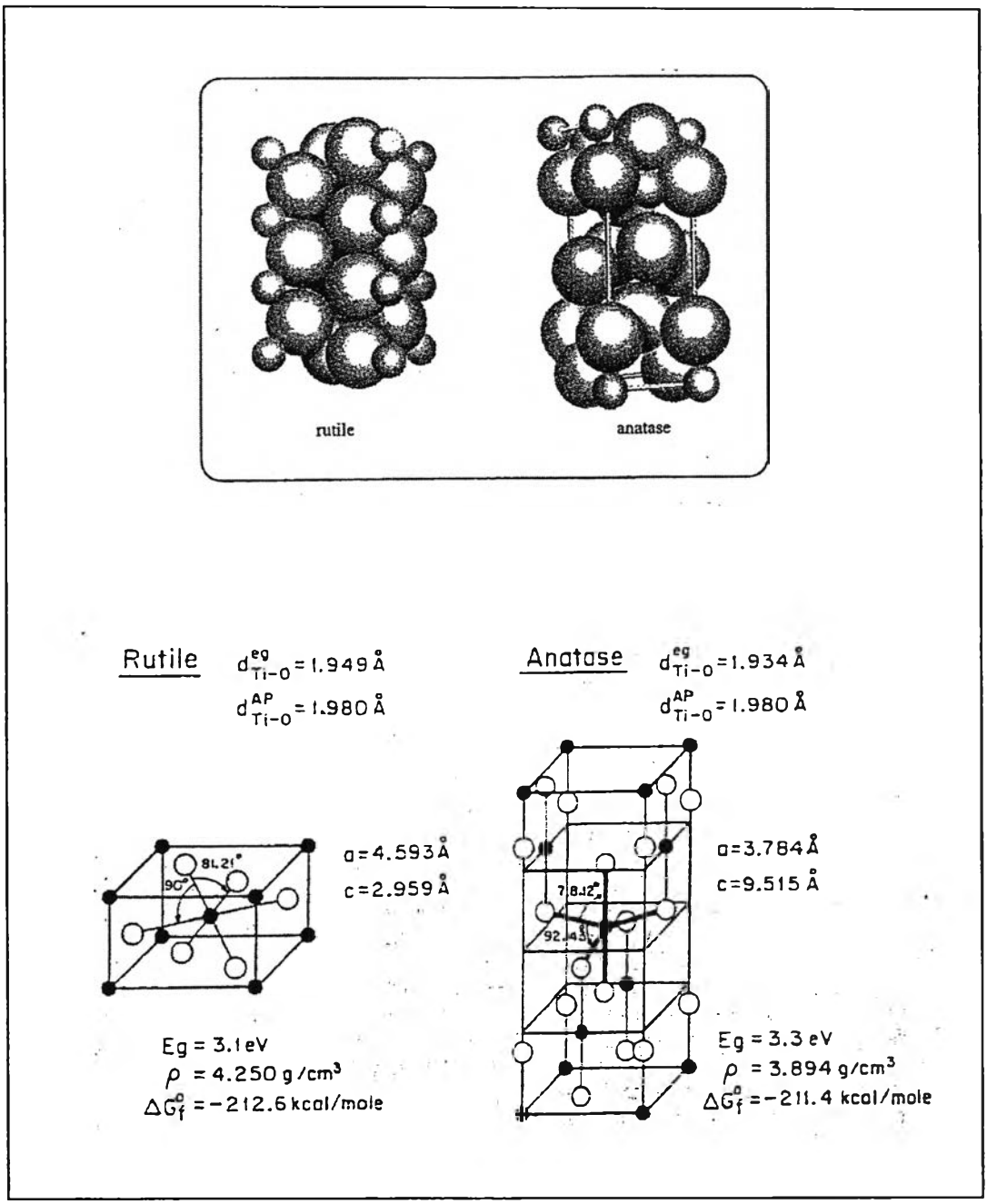

Figure 2.3 Crystal structure of TiO_2: rutile and anatase (Linsebigler et al., 1995; Fujishima et al., 1999)

Table 2.1 Comparison of rutile and anatase (Linsebigler et al., 1995 and Fujishima et al., 1999)

Property	Rutile	Anatase
Crystalline form	Orthorhombic	Orthorhombic
Band gap energy (eV)	3.030	3.200
Hardness (Mohs)	6.0-7.0	5.5-6.0
Density (g/cm^3)	4.250	3.894
Gibbs free energy, ΔG_f° (kcal/mole)	-212.6	-211.4
Lattice constant, a (Å)	4.593	3.784
Lattice constant, c (Å)	2.959	9.515
Melting point	1858 °C	Changes to rutile at high temperature ~ 800 °C

The anatase polymorph of TiO_2 apparently shows higher photoactivity than rutile. Besides the difference in structure, the energy band structure and surface chemistry are key factors. The band gap energy of anatase is 3.2 eV, which corresponds to UV light (388 nm), while the band gap energy for rutile is 3.0 eV corresponding to violet light (413 nm). The difference in band gap comes from the level of conduction band edge of anatase which is higher than that of rutile by about 0.2 eV. Thus, electrons from the conduction band of anatase have higher reducing power than those of rutile (Fujishima et al., 1999).

Titanium dioxide (TiO_2) in a photocatalytic system is used as a fine powder or as a thin film. The TiO_2 powder is widely used in both laboratory and pilot plant scale in the form of slurry or aqueous suspension. This TiO_2 type offers the advantage of high surface dispersion and, consequently, optimization of the encounter frequency of the active surface of a photocatalyst with a pollutant substrate. Use of the powder form has a disadvantage in commercial-scale operations due to the need for post treatment to remove the powder from the treated water. The TiO_2 thin film is deployed to solve those problems by fixing the photocatalyst powder on solid materials such as hollow glass beads, hollow tubes, woven fabric, silica gel, and sand (Matthews, 1986; Matthews and McEvoy, 1992; Fujishima et al., 1999). Besides the ease of handling the photocatalyst after use in the reactor, this modification provides

the advantage of bias potential application to the photocatalyst film to separate the photogenerated carriers, thereby improving photocatalytic efficiency. However, in general, this TiO_2 modification results in lower photocatalytic activity relative to the slurry or suspension form due to its smaller contact area, and greater susceptibility to poisoning and permanent deactivation (Fujishima et al., 1999).

Recently, most research is focused on modifying the TiO_2 structure to improve TiO_2 properties for various applications. The production of TiO_2 particles with a specific size and morphology is of primary importance for the development of this material. Since the photocatalytic activity for environmental applications is mostly confined to the surface of the photocatalytic material, its surface area must be increased to maximize the photocatalytic activity. One way to do this is the synthesis of nano-sized TiO2 particles to increase photocatalytic reaction sites on the surface. Also, the amount of the anatase phase must be maximized because the rutile phase shows less photocatalytic activity (Asashi et al., 2001)

2.3 Sol-gel process

Sol–gel processing is one of the most common methods to produce photocatalyst TiO2 in both forms of coatings and powder. *Sols* are dispersions of colloidal particles in a liquid. *Colloids* are solid particles with diameters of 1-100 nm (Davis and Rideal, 1963). A *gel* is an interconnected, rigid network with pores of submicrometer dimensions and polymeric chains whose average length is greater than a micrometer.

Steps and details of sol-gel preparation are illustrated in Figure 1 and can be described as follow (Hench and West, 1990):

- Forming a gel by network growth from an array of discrete colloidal particles or by formation of an interconnected 3-D network by the simultaneous hydrolysis and polycondensation of an organometallic precursor.
- Removing of the pore liquid as a gas phase from the interconnected solid gel network under hypercritical conditions, the network does not collapse and a low density *aerogel* is produced. Aerogels can have pore volumes as large as 98% and densities as low as 80 kg/m (Fricke and Capo, 1988).

- In an alternative way, removing of pore liquid at or near ambient pressure by thermal evaporation, called *drying,* and shrinkage occurs, the monolith is termed a *xerogel.* If the pore liquid is primarily alcohol based, the monolith is often termed an *alcogel*
- A gel is defined as *dried* when the physically adsorbed water is completely evacuated. This occurs between 100 and 180 °C. The surface area of dried gels may be very large (>400 m^2/g), and the average pore radius very small (<10 nm). Larger pore radii *can* be produced by thermal treatment (West et al., 1988), by chemical washing during aging (Wilson, 1989) or by additions of HF to the sol.
- A dried gel still contains a very large concentration of chemisorbed hydroxyls on the surface of the pores. Thermal treatment in the range 500-800 °C desorbs the hydroxyls and thereby decreases the contact angle and the sensitivity of the gel to rehydration stresses, resulting in a *stabilized gel.*
- Elevating temperatures to reduce the number of pores and their connectivity due to viscous-phase sintering. This is termed *densification.* The density of the monolith increases and the volume fraction of porosity decreases during sintering.
- The porous gel is transformed to a dense material when all pores are eliminated. Densification is complete either at 1250-1500 °C for gels or as low as 1000 °C depending on the preparation method (Klein and Garvey, 1984). The densification temperature decreases as the pore radius decreases and surface area of the gels increases.

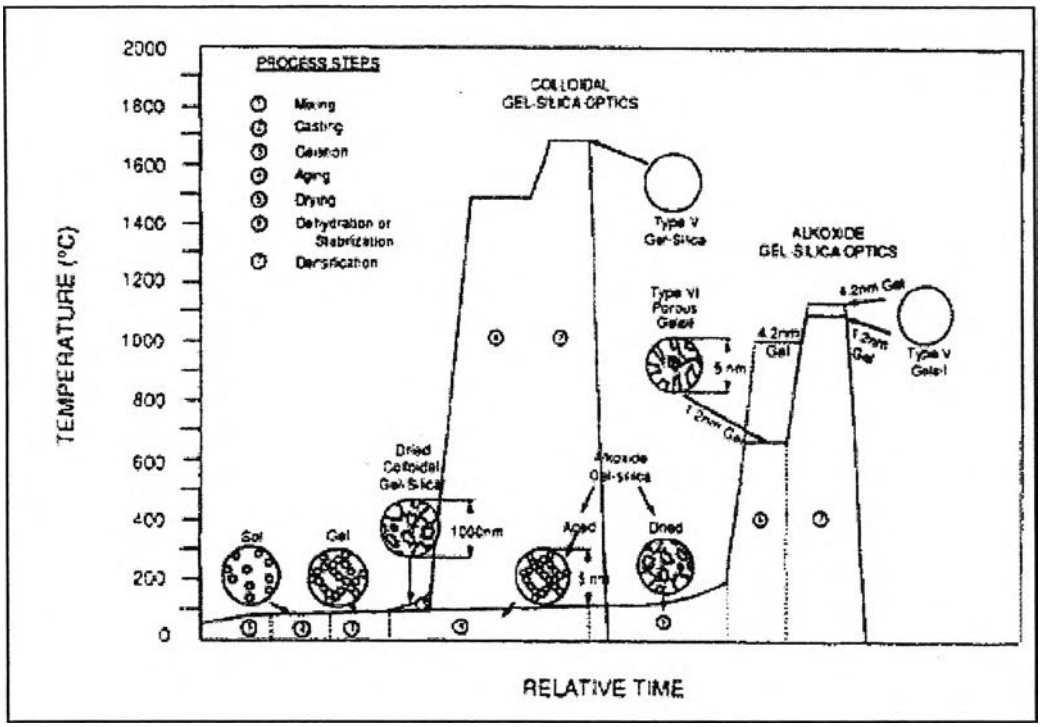

Figure 2.4 Forming of various types of crystals in Sol-gel processes

In summary, the sol-gel process includes four steps: hydrolysis, polycondensation, drying, and thermal decomposition.

Equations relating to the reaction of sol-gel process are summarized below. Precursors of the metal or nonmetal alkoxides hydrolyze with water or alcohols according to the hydrolysis process as shown by Equation (2.9):

$$M(OR)_x + mH_2 \rightarrow M(OR)_{x-m}(OH)_m + m\text{ROH} \qquad (2.9)$$

where if m is up to x, the reaction is total hydrolysis.

The water and alcohol condensations are shown by Equation (2.10) and (2.11), respectively:

$$2M(OR)_{x-m}(OH)_m \rightarrow (OH)_{m-1}(OR)_{x-m}\text{-M-O-M}(OR)_{x-m}(OH)_{m-1} + H_2O \qquad (2.10)$$

$$2M(OR)x\text{-}m(OH)m \rightarrow (OH)m\text{-}1(OR)x\text{-}m\text{-M-O-M}(OR)x\text{-}m\text{-}1 + ROH \qquad (2.11)$$

The overall reaction can be expressed as Equation (2.12):

$$M(OR)_x + {}^{x}/_{2}H2O \rightarrow MO_{x/2} + xHOR \quad (2.12)$$

In addition to water and alcohol, an acid or a base can also help to hydrolyze the precursor. In the case of an acid, a reaction takes place between alkoxide and the acid as shown in Equation (2.13):

$$-M-OR + AOH \rightarrow -M-O-A + ROH \quad (2.13)$$

After the solution has been condensed to a gel, the solvent must be removed. Higher temperature calcinations is needed to decompose the organic precursor.

The role of the stabilizing agent on nanocrystal size powder is well described by Burda et al. (2005). Various organic and inorganic materials have been utilized to improve the nanoparticle properties such as capping materials on the surface of nanoparticles through covalent or ionic interactions. The surface plays an important role in the properties of nanoparticles, including the solubility, reactivity, stability, melting point, and electronic structure.

Examples of stabilizing agents using in the surface improvement of TiO_2 include acetyl acetone (Kajitvichyanukul et al., 2005 (a)), diethanoloamine (Kajitvichyanukul and Jirapattarasakul, 2005), and surfactants (Sakulkhaemaruethai et al., 2005). However, less study is focused on using polymer especially ethylene glycol as stabilizing agent to enhance nanoparticle properties. Some previous work is mainly focused on using polyethylene glycol (Kajitvichyanukul and Amornchat, 2005; Kajitvichyanukul et al., 2005(b)) which exhibits a good stabilizing agent in improving adhesive property and maintaining photocatalytic activity of TiO_2 thin film immobilized on stainless steel. In this work two types of ethylene glycol were selected, which are diethylene glycol (DEG) and polyethylene glycol (PEG). These two stabilizing agents will be investigated and compared for the effects of the short and long chains of ethylene glycol polymers on TiO_2 nanoparticle properties as well as photocatalytic activity in chromium (VI) removal.

2.4 Chromium

2.4.1 Sources and Properties

Chromium is a naturally occurring element in rocks, animals, plants, soil, and volcanic dust and gases. In form of a metal, it is a steel-gray solid with a high melting point and an atomic weight of 51.996 g/mol (ASTDR, 1998). The oxidation states of chromium are ranging from chromium (-II) to chromium (+VI). The trivalent chromium (Cr III) and hexavalent chromium (Cr VI) are the predominant species of chromium in the environment. The trivalent chromium (Cr III) occurs naturally and is an essential nutrient. The trivalent chromium salts such as chromium polynicotinate, chromium chloride and chromium picolinate (CrP) are used as micronutrients and nutritional supplements and have been demonstrated to exhibit a significant number of health benefits in animals and humans (Anderson, 2000)

The hexavalent chromium, which, along with the less common metallic chromium (III), is most commonly produced by industrial processes. The most important industrial sources of chromium in the atmosphere are those related to ferrochrome production. Ore refining, chemical and refractory processing, cement-producing plants, automobile brake lining and catalytic converters for automobiles, leather tanneries, and chrome pigments also contribute to the atmospheric contribution of chromium. (USEPA, 1998(a)). The metal chromium is used mainly for making steel and other alloys (ASTDR, 1998). Chromium compounds, in either the chromium (III) or chromium (VI) forms, are used for chrome plating, the manufacture of dyes and pigments, leather and wood preservation, and treatment of cooling tower water. Smaller amounts are used in drilling muds, textiles, and toner for copying machines (ASTDR, 1998)

Chromium forms a large number of compounds, in both the chromium (III) and the chromium (VI) forms. Chromium compounds are stable in the trivalent state, with the hexavalent form being the second most stable state (ASTDR, 1998). The chromium (III) compounds are sparingly soluble in water and may be found in water bodies as soluble chromium (III) complexes, while the chromium (VI) compounds are readily soluble in water.

2.4.2 Toxicology Data

2.4.2.1 Exposure pathway of chromium

The reduction of Cr(VI) to Cr(III) results in the formation of reactive intermediates that contribute to the cytotoxicity, genotoxicity and carcinogenicity of Cr(VI)-containing compounds. In general, humans are exposed to chromium (generally chromium [III]) by eating food, drinking water, and inhaling air that contains the chemical. The average daily intake from air, water, and food is estimated to be less than 0.2 to 0.4 micrograms (μg), 2.0 μg, and 60 μg, respectively (ASTDR, 1998). Dermal exposure to chromium may occur during the use of consumer products that contain chromium, such as wood treated with copper dichromate or leather tanned with chromic sulfate (ASTDR, 1998) Chromium enters the body through the lungs, gastro-intestinal tract and to a lesser extent through skin. Inhalation is the most important route for occupational exposure, whereas non-occupational exposure occurs via ingestion of chromium-containing food and water. Regardless of the route of exposure Cr (III) is poorly absorbed whereas Cr (VI) is more readily absorbed. Further, absorption of Cr (VI) is poorer by the oral route, it is thus not very toxic when introduced by the oral route. But chromium is very toxic by dermal and inhalation routes and causes lung cancer, nasal irritation, nasal ulcer, hypersensitivity reactions and contact dermatitis. All the ingested Cr (VI) is reduced to Cr (III) before entering in the blood stream. Cr (III) is unable to enter into the cells but Cr (VI) enters through membrane anionic transporters. Intracellular Cr (VI) is metabolically reduced to Cr (III). Cr (VI) does not react with macromolecules such as DNA, RNA, proteins and lipids. However, both Cr (III) and the reductional intermediate Cr (V) are capable of co-ordinate.

2.4.2.2 Acute effect of chromium

Chromium (VI) is much more toxic than chromium (III), for both acute and chronic exposures (ASTDR, 1998; USEPA, 1998 (a) and (b)). The respiratory tract is the major target organ for chromium (VI) following inhalation exposure in humans. Shortness of breathes, coughing, and wheezing were reported in cases where an individual inhaled very high concentrations of chromium trioxide. Ingestion of high amounts of chromium (VI) causes gastrointestinal effects in humans and animals, including abdominal pain, vomiting, and hemorrhage (ASTDR, 1998). Acute animal tests have shown chromium (VI) to have extreme toxicity from inhalation and

oral exposure. For chromium (III), the moderate toxicity from oral exposure is found from animal tests (ASTDR, 1998).

2.4.2.3 Chronic effect of chromium

Chronic inhalation exposure to chromium (VI) in humans results in effects on the respiratory tract, with perforations and ulcerations of the septum, bronchitis, decreased pulmonary function, pneumonia, asthma, and nasal itching and soreness reported (USEPA, 1998(b)). Chronic human exposure to high levels of chromium (VI) by inhalation or oral exposure may produce effects on the liver, kidney, gastrointestinal and immune systems, and possibly the blood. Dermal exposure to chromium (VI) may cause contact dermatitis, sensitivity, and ulceration of the skin. (ASTDR, 1998; USEPA, 1998(b)). The Reference Concentration (RfC) for chromium (VI) (particulates) is 0.0001 mg/m^3 based on respiratory effects in rats. The Reference Concentration (RfC) for chromium (VI) (chromic acid mists and dissolved Cr (VI) aerosols) is 0.000008 mg/m^3 based on respiratory effects in humans (USEPA, 1999(a)). EPA has low confidence in the RfC based on low confidence in the study on which the RfC for chromium (VI) (chromic acid mists and dissolved Cr (VI) aerosols) is based.

The Reference Dose RfD for chromium (VI) is 0.003 mg/kg/d based on the exposure at which no effects were noted in rats exposed to chromium in the drinking water (USEPA, 1999 (a)). EPA has low confidence in the RfD based on low confidence in the study on which the RfD for chromium (VI) was based because a small number of animals were tested, a small number of parameters were measured, and no toxic effects were noted at the highest dose tested; and low confidence in the database because the supporting studies are of equally low quality and developmental endpoints are not well studied.

For chromium III, although data from animal studies have identified the respiratory tract as the major target organ for chronic chromium exposure, these data do not demonstrate that the effects observed following inhalation of chromium (VI) particulates are relevant to inhalation of chromium (III) (USEPA, 1999 (b)). EPA has not established an RfC for chromium (III). The RfD for chromium (III) is 1.5 mg/kg/d based on the exposure level at which no effects were observed in rats exposed to chromium (III) in the diet(USEPA, 1999 (b). EPA has low confidence in the RfD based on: low confidence in the study on which the RfD for chromium (III) was based

due to the lack of explicit detail on study protocol and results; and low confidence in the database due to the lack of high-dose supporting data (USEPA, 1999 (b).

Epidemiological studies of workers have clearly established that inhaled chromium is a human carcinogen, resulting in an increased risk of lung cancer. Although chromium-exposed workers were exposed to both chromium (III) and chromium (VI) compounds, only chromium (VI) has been found to be carcinogenic in animal studies, so EPA has concluded that only chromium (VI) should be classified as a human carcinogen (USEPA, 1999 (a)). EPA has classified chromium (VI) as a Group A, known human carcinogen by the inhalation route of exposure. For chromium (III), there is no data available on the carcinogenic potential of chromium (III) compounds alone (USEPA, 1999(b)). EPA has classified chromium (III) as a Group D, not classifiable as to carcinogenicity in humans. EPA has stated that "the classification of chromium (VI) as a known human carcinogen raises a concern for the carcinogenic potential of chromium (III) (USEPA, 1999(b)).

2.5 Chromium removal by the photocatalysis process

The photocatalytic reduction of Cr (VI) in aqueous suspensions of semiconductors such as TiO_2, ZnO, CdS, ZnS, and WO_3 under UV illumination has been widely studied (Dom`enech, J., and Mu˜noz, 1987; Prairie, 1993; Nav´ıo, 1998) and constitutes the basis of promising new decontamination technologies. It has also been shown that the photocatalytical reduction of Cr (VI) in aqueous suspensions of ZnO can take place under sunlight (3). The optimum conditions to treat chromium using TiO_2 was well established from the previous works (Kajitvichyanukul and Watcharenwong, 2005; Ku, 2001). It was found that Cr (VI) was well removed from wastewater at the reaction pH of 3. The efficiency in Cr (VI) removal can be enhanced with the addition of hole scavenger (for example; formate ions) which eliminate the recombination effect. The photocatalytic reduction rate of Cr (VI) was found to be linearly increased with light intensity until a certain optimum light intensity was reached (Ku, 2001).

In this work, as the tested pollutant, Cr (VI) is selected to compare the removal efficiencies using various types of nanoparticle preparing from different conditions. The optimum condition in treating Cr (VI) was transferred from the previous work (Kajitvichyanukul and Watcharenwong, 2005) and photocatalytic reduction of Cr (VI)

was at the focus. As already published, the mechanism of Cr (VI) removal is not included in this purposed research work.